GEOLOGY

Paleo–salt water dominates coastal aquifer salinization: A continental-scale study in China

Tianyuan Zheng[1,2], Bo Guo[3], Qinpeng Chang[1,2], Qiguo Sun[4], Xiaogang Chen[5], Xilai Zheng[1,2]*, Jichun Wu[6], Zhihong Zheng[1,2], Shaobo Gao[1,2], Chunmiao Zheng[7,8], Junguo Liu[7,9], Dong Wang[1,2], Tao Liu[1,2], Xiaolei Liu[1,2], Guangquan Chen[10]*, Xingyong Xu[11], Bo Zhang[12], Lin Zhang[1,2], Yajie Wu[13], Olaf Kolditz[14], Jian Luo[15]*, Alberto Guadagnini[16]

Seawater intrusion poses a major threat to freshwater resources in coastal aquifers worldwide. In China alone, these types of aquifers provide a vital groundwater source for nearly 400 million people. Whereas modern seawater intrusion is often attributed to human activities and climate change, the role of paleo–salt water remains poorly quantified. This continental-scale investigation of seawater intrusion in China reveals that paleo–salt water, not modern seawater, dominates salinity patterns in large sedimentary basins. Analysis of over 2100 water samples shows a strong correlation between intrusion and tectonic subsidence zones, with paleo–salt water affecting 66% of the observed salinized areas. In northern coastal plains, paleo–salt water trapped in confined aquifers is characterized by salinity levels exceeding 144.6 grams per liter, whereas modern seawater intrusion (34%) occurs in hilly regions with thinner sediments. Isotopic signatures ($\delta^{18}O$) trace paleo–salt water intrusion to Quaternary sea level changes. These findings improve seawater intrusion source identification and inform global salinity management.

INTRODUCTION

Groundwater is a vital freshwater resource for billions worldwide, particularly in densely populated coastal regions where it supports agricultural, industrial, and domestic water demands (*1*–*5*). However, this critical resource is increasingly threatened by seawater intrusion, a widespread geologic hazard that degrades water quality and endangers coastal communities (*6*–*9*). Seawater intrusion occurs when saline water migrates into freshwater aquifers due to excessive groundwater withdrawal, natural geologic processes, or a combination of both (*2*, *3*, *10*). In addition, climate change (*11*), land use changes (*12*), and declining recharge rates (*2*, *11*) have further exacerbated the problem, making it a growing global concern.

Among the regions most affected by seawater intrusion, China faces particularly acute challenges due to its rapid industrialization and heavy reliance on groundwater (*13*). Groundwater supports over 400 million people in China (*14*–*16*), with northern coastal regions such as Jiaozhou Bay, Qinhuangdao, and Longkou experiencing notable seawater intrusion (*17*). The issue was first documented in 1964 in Liaodong Bay (*18*) and has since intensified, particularly in areas where shallow phreatic aquifers are overexploited for irrigation and public water supplies (*17*). Northern China, characterized by low rainfall and extensive plains, is especially vulnerable due to intensive industrial and agricultural groundwater extraction (*17*). Despite the growing severity of seawater intrusion, existing research has largely been site specific, lacking a systematic, continental-scale investigation to understand regional patterns and underlying drivers.

Whereas modern seawater intrusion is commonly attributed to human activities, a more complex and long-term challenge arises from the presence of paleo–salt water remnants of ancient marine transgressions that remain trapped within aquifers (*19*–*23*). Origins of this paleo–salt water are linked to Quaternary sea level fluctuations, where cycles of marine transgressions and regressions deposited low-permeability sediments that trapped seawater in coastal aquifers (*24*–*26*). Coastal studies have revealed high-salinity retention from past sea level fluctuations (*27*–*30*), complicating efforts to distinguish recent seawater intrusion from inherited salinity (*19*–*22*). In China, geological surveys have identified high-salinity groundwater along the Bohai Sea coast (*31*–*33*), with salinity levels in some regions exceeding 144.6 g/liter (*34*). During periods of sea level regression, dating to about 70,000 to 39,000 years ago (*17*), the Bohai Sea transformed into a vast closed salt lake, where intense evaporation created highly saline groundwater (*35*). Similar patterns have been observed in the coastal aquifers of North Jiangsu near the Yellow Sea and the Zhujiang River delta near the South China Sea (*23*, *36*). These findings suggest that, beyond active intrusion from the ocean, paleo–salt water stored in deep aquifers may be a notable but

[1]College of Environmental Science and Engineering, Ocean University of China, Qingdao 266100, P. R. China. [2]Key Laboratory of Marine Environment and Ecology, Ministry of Education, Ocean University of China, Qingdao 266100, P. R. China. [3]Department of Hydrology and Atmospheric Sciences, University of Arizona, Tucson, AZ 85721, USA. [4]School of Computer Science and Engineering, Jiangsu University of Science and Technology, Zhenjiang 212003, P. R. China. [5]Key Laboratory of Coastal Environment and Resources of Zhejiang Province, School of Engineering, Westlake University, Hangzhou 310024, P. R. China. [6]School of Earth Sciences and Engineering, Nanjing University, Nanjing 210093, P. R. China. [7]State Environmental Protection Key Laboratory of Integrated Surface Water-Groundwater Pollution Control, Guangdong Provincial Key Laboratory of Soil and Groundwater Pollution Control, School of Environmental Science and Engineering, Southern University of Science and Technology, Shenzhen 518055, P. R. China. [8]Eastern Institute for Advanced Study, Eastern Institute of Technology, Ningbo 315201, P. R. China. [9]Henan Provincial Key Lab of Hydrosphere and Watershed Water Security, North China University of Water Resources and Electric Power, Zhengzhou 450046, P. R. China. [10]Key Laboratory of Marine Sedimentology and Environmental Geology, First Institute of Oceanography, Ministry of Natural Resources, Qingdao 266061, P. R. China. [11]Guangxi Key Laboratory of Beibu Gulf Marine Resources, Environment and Sustainable Development, Fourth Institute of Oceanography, Ministry of Natural Resources, Beihai 536015, P. R. China. [12]College of Earth Science and Engineering, Shandong University of Science and Technology, Qingdao 266590, P. R. China. [13]College of Engineering, Ocean University of China, Qingdao 266100, P. R. China. [14]Helmholtz Centre for Environmental Research–UFZ, Permoserstraße 15, Leipzig 04318, Germany. [15]School of Civil and Environmental Engineering, Georgia Institute of Technology, Atlanta, GA 30332, USA. [16]Department of Civil and Environmental Engineering, Politecnico di Milano, Milano 20156, Italy.
*Corresponding author. Email: zhxilai@ouc.edu.cn (X.Z.); chenguangquan@fio.org.cn (G.C.); jian.luo@ce.gatech.edu (J.L.)

poorly understood contributor to salinization (*37*–*39*). However, the relative contributions of modern seawater and paleo–salt water remain unresolved, limiting our ability to develop effective groundwater management strategies.

To address this critical knowledge gap, we present the comprehensive, nationwide investigation of seawater intrusion along China's coastline. We hypothesize that tectonic subsidence zones play a fundamental role in controlling seawater intrusion patterns, with paleo–salt water being a dominating factor in large sedimentary basins. Our study aims to (i) establish large-scale correlations between seawater intrusion and geological structures, (ii) quantify spatial and temporal changes in salinity and groundwater levels across fresh, saline, and brine aquifers, and (iii) assess the role of paleo–salt water in salinization through geochemical analyses. By integrating extensive field data, geophysical surveys, and geochemical tracers, this research provides a critical framework for understanding seawater intrusion mechanisms at a continental scale, with implications for managing coastal groundwater resources globally.

RESULTS AND DISCUSSION

Patterns of seawater intrusion controlled by tectonics

Our analysis of seawater intrusion patterns rests on an extensive hydrogeological dataset, the key elements of the methodology associated with its collection and curation being detailed in the Materials and Methods section. To delineate tectonic controls on seawater intrusion, Fig. 1 synthesizes main spatial data, including the distributions of main lithological types, paleo-saltwater boundaries, and sampling well locations along the coast. On the basis of this synthesis, we exemplify the characterization of the system through

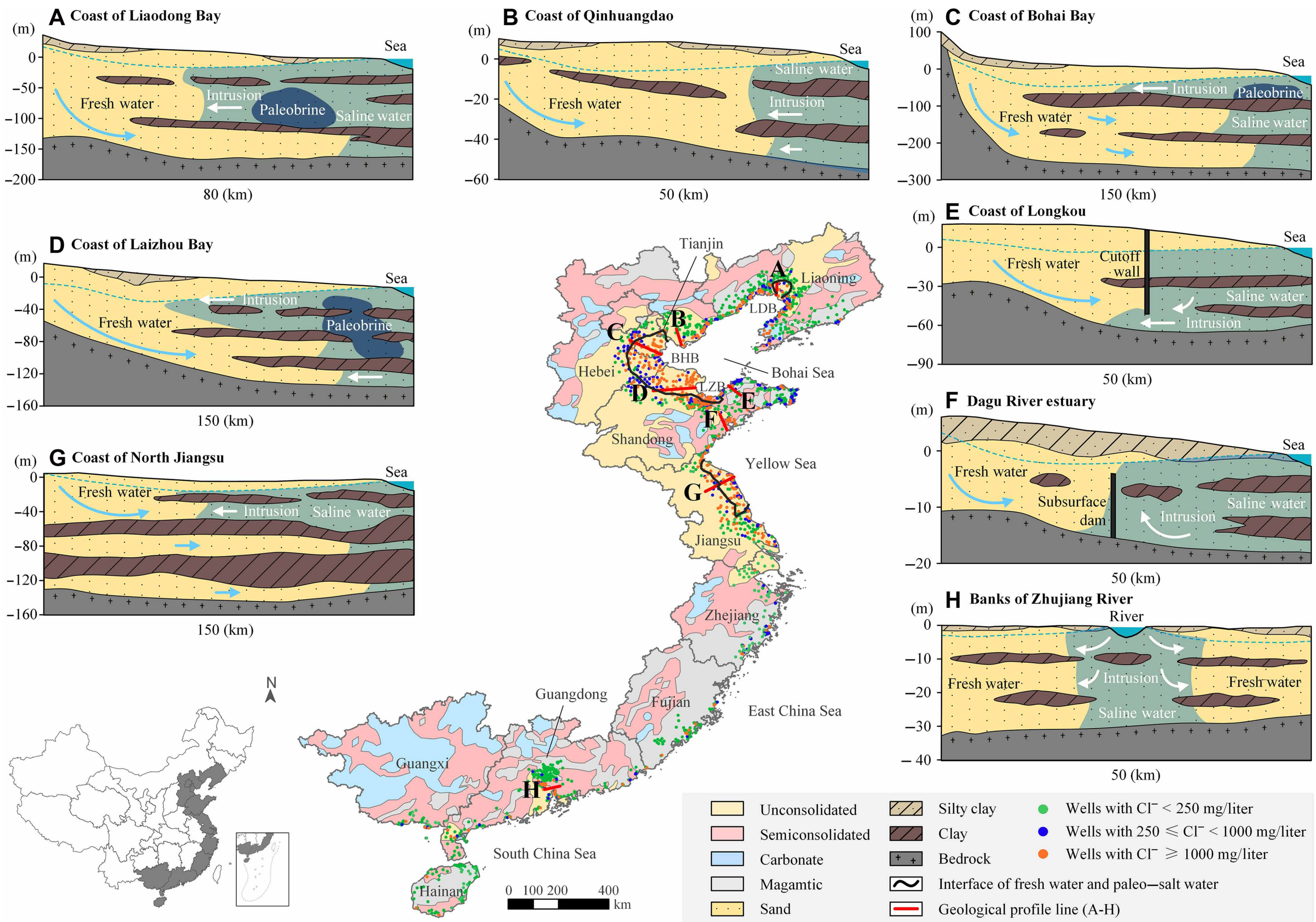

Fig. 1. Distributions of paleo–salt water and monitoring wells along the coastal areas of China. Graphical depiction of hydrogeological cross sections of seawater intrusion within areas associated with transects highlighted in red. (**A**) In the Liaodong Bay (LDB), the first seawater intrusion was documented in 1964 as a consequence of groundwater pumping; (**B**) in Qinhuangdao, seawater intrusion was detected in 1975 due to a combination groundwater overextraction and limited recharge (*60*); (**C**) along the coastline of the Bohai Bay (BHB), high groundwater withdrawals caused groundwater levels to drop below sea level, thus aggravating paleo-saltwater intrusion (*61*); (**D**) in the Laizhou Bay (LZB), extensive groundwater withdrawals for irrigation and chemical plants lowered groundwater levels and induced the most severe paleo-saltwater intrusion documented in China (*54*, *62*); (**E**) in Longkou, high volumes of groundwater withdrawals caused seawater intrusion and an underground cutoff wall was built as a control measure; (**F**) in the Dagu River estuary, seawater intrusion began in 1970 (*63*) and extended for about 20 km (installation of a subsurface dam has mitigated intrusion of modern seawater in the phreatic aquifer); (**G**) in North Jiangsu, groundwater overpumping caused paleo-saltwater intrusion in unconfined and shallow confined aquifers (*45*); (**H**) on the banks of Zhujiang River, seawater upflow following the tides along the Zhujiang River induced modern seawater intrusion (*64*).

hydrogeological cross sections encompassing eight typically documented seawater intrusion areas (Fig. 1), which we detail in the following. Aquifer systems in the coastal regions are chiefly composed of single or multiple porous formations underlain by bedrock formations. Seawater intrusion is most prominent along the coastal areas of Northern China (including Liaoning, Hebei, Shandong, Jiangsu provinces, and Tianjin municipality). It is also detected along the coastlines of Zhejiang, Fujian, Guangxi, Hainan, and Guangdong provinces. In situ investigations unveil a notable alignment between the patterns of seawater intrusion and of the main geological structures across China (Fig. 1). These areas are characterized by subsidence zones in the Liaodong Bay, Bohai Bay, Laizhou Bay, and North Jiangsu (Fig. 1, A, C, D, and G), as well as uplift zones in Qinhuangdao, Longkou, the Jiaozhou Bay (Dagu River estuary), and the Zhujiang estuary (Fig. 1, B, E, F, and H).

Three clearly identified subsidence zones correspond to the coastal plains of Liaodong Bay, North China (encompassing the Bohai Bay and Laizhou Bay) and North Jiangsu. According to sedimentological data associated with wellbore drilling and water quality investigations, the coastal porous aquifer systems are composed of alluvial and deltaic sediments. These Quaternary sediments and river paleochannels constitute a multilayered aquifer-aquitard system. Several interbedded fine-grained marine sediments are also hosted in the coastal regions (*24*). Fresh groundwater is mainly distributed in the inland diluvium-alluvial and alluvial areas, whereas paleo–salt water is found within one unconfined aquifer and one to three confined aquifers (these being separated by semipermeable or impervious layers). The fresh groundwater and paleo–salt water have been highly exploited over the past decades for various purposes, groundwater levels being documented to suffer from a continuous decline. The latter is particularly strong in the coastal plains of Northern China.

In contrast, three uplift zones align with hilly and mountainous coastal regions of Liaodong Peninsula, Shandong Peninsula (including Longkou and Dagu River estuary), and Southern China (as depicted in the central maps of Fig. 1). In these areas, the internal architecture of the coastal aquifers mainly comprises Quaternary sediments. Groundwater is mainly hosted in aquifers characterized by a generally low overall specific capacity. Otherwise, one can notice the presence of some discontinuous coastal aquifers along river corridors. These are often composed of thin sand layers (10 to 30 m thick), as observed in the Pearl River estuary, where seawater intrusion takes place in the Quaternary porous aquifers on both riverbanks. To prevent and control seawater intrusion, eight subsurface barriers [comprising subsurface dams (*40*) (Fig. 1F) and cutoff walls (*41*) (Fig. 1E)] have been placed since 1985 in the unconfined aquifers around the Shandong Peninsula.

Meteorological and hydrological factors exert varying degrees of influence on the occurrence and progression of seawater intrusion (*6*, *42*, *43*). Under global warming, sea level along the coast of China has exhibited a fluctuating upward trend, rising at an average annual rate of 3.4 mm between 1980 and 2021. The continuous sea level rise alters the balance of the groundwater-seawater interface and contributes to intensifying seawater intrusion into aquifer systems (*3*). Seasonal and long-term temperature fluctuations may further alter exchange dynamics between aquifers and the ocean, whereas seawater warming can enhance tidal-driven circulation in the upper intertidal zone. Frequent storm surges in coastal regions prolong seawater retention near shorelines, occasionally inundating farmland and creating favorable conditions for seawater intrusion. In addition, it can be noted that many rivers in coastal areas such as Liaodong Bay, Qinhuangdao, Bohai Bay, Laizhou Bay, and Longkou are seasonal due to flat topography, limited rainfall, and short flow paths. During dry periods, runoff decreases markedly and rivers may even dry up for prolonged periods, thus allowing seawater to intrude upstream along the rivers. Similarly, surface discharge associated with rivers along the Pearl River substantially decreases and, during the ebb tides (particularly under storm tide conditions), seawater propagates upstream along the rivers, causing saltwater intrusion along both banks of the rivers (Fig. 1H).

Human activities represent another critical driver of seawater intrusion. Excessive groundwater extraction in coastal plains has generated depression cones, thus contributing to reverse natural hydraulic gradients and inducing intrusion of both modern seawater and paleo–salt water across extensive coastal zones (Fig. 1, A to H). Moreover, seawater, saline groundwater, and brine are often extracted and transported inland (for distances ranging from hundreds of meters to several kilometers) for coastal aquaculture and salt production. When such practices are carried out without adequate impermeable barriers, they further exacerbate local saltwater intrusion.

Compared with the China Marine Ecological Status Bulletin (2011 to 2017), the overall trend of seawater intrusion in China has been relatively stable over the past 10 years, and no substantial increase in the distance of seawater intrusion. However, the distances of paleo-saltwater intrusion have decreased in the coastal regions of Bohai Bay, Laizhou Bay, and North Jiangsu due to the restriction on the freshwater exploitation of deep confined aquifer. On the contrary, the distances of seawater intrusion have extended slightly in the coastal areas of Longkou and Zhujiang River Estuary because of the increase in the extraction of underground fresh water.

In summary, one can note that seawater intrusion in coastal areas is governed by both natural processes and human activities. Geological structures define the fundamental framework that controls intrusion patterns, whereas meteorological and hydrological factors shape its pathways, types, and spatial distribution. In contrast, unsustainable human activities accelerate the rate and expand the extent of seawater intrusion.

Dynamics of chloride (Cl^-) concentrations and water table

The Cl^- concentration is strongly correlated to salinity, and its analysis is often used to describe seawater intrusion (*44*). Marked space-time dynamics of Cl^- concentration are evidenced at the scale analyzed, the corresponding values ranging between 0.49 and 97432.97 mg/liter (with a mean of 2480.16 mg/liter and a median of 193.57 mg/liter). We note that current national standards in China rely on values of Cl^- concentrations in groundwater to quantify severity of seawater intrusion. According to these standards, seawater presence in groundwater is typically classified according to three categories, i.e., absent ($Cl^- \leq$ 250 mg/liter), mild ($1000 \geq Cl^- > 250$ mg/liter), and severe ($Cl^- \geq$ 1000 mg/liter) (*45*, *46*). Our extensive sampling campaign (see table S1) documents that low-salinity groundwater accounts for 37.69% of the total samples and is chiefly located within inland shallow aquifers (Fig. 2). This distribution reflects the recharge efficiency of rainfall and the contribution of runoff recharge in these areas. Otherwise, medium- and high-salinity groundwater (which is primarily found in the nearshore regions) constitutes 62.31% of the total. To provide insights into seawater intrusion dynamics, we analyze Cl^- concentration and groundwater level changes across eight representative coastal regions in Fig. 2, as described in the following. The eight representative coastal

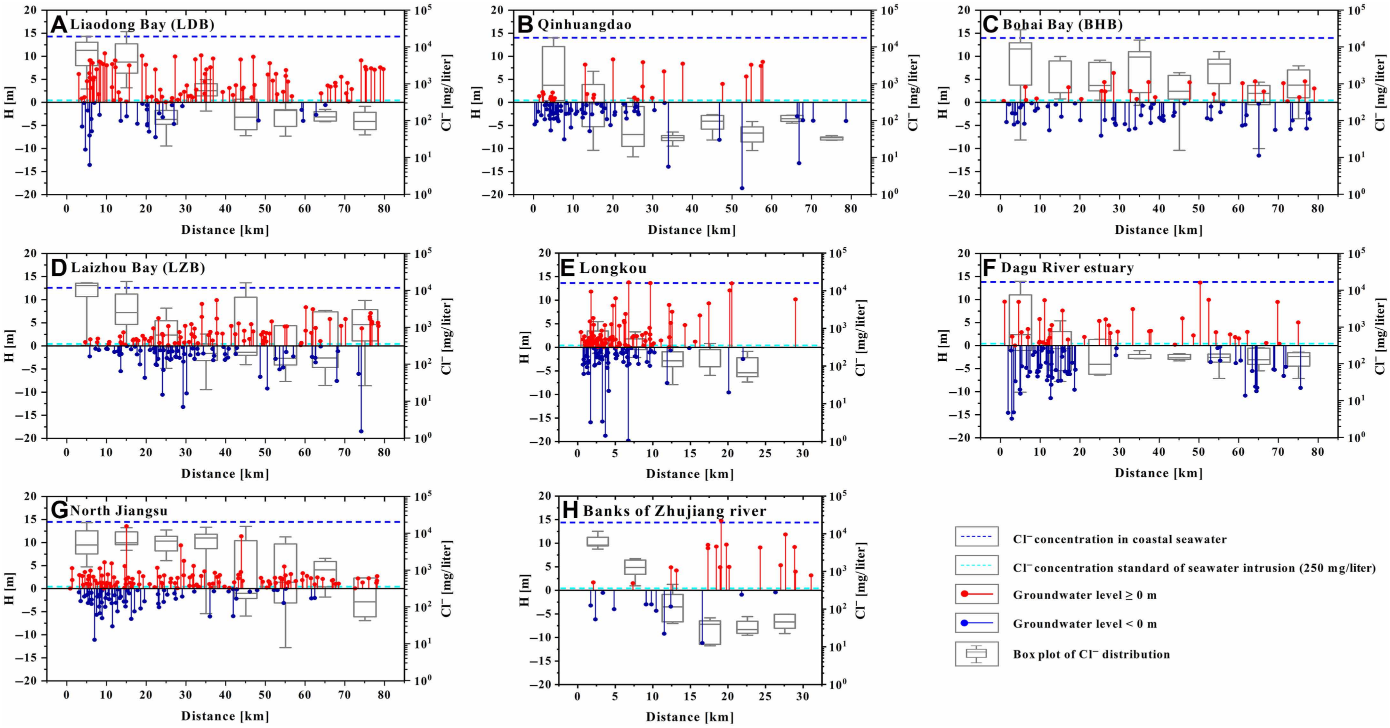

Fig. 2. Groundwater levels and Cl⁻ concentrations versus distance from the coast. Each panel (**A** to **H**) depicts sampled levels (H, given in meters above sea level) of water table and distributions of Cl⁻ concentrations as a function of distance from coastline. Red or blue vertical bars correspond to sampled water table values higher and equal to or lower than zero (i.e., higher and lower than sea level), respectively. Box plots represents Cl⁻ distributions within given interval distances at each of the eight areas analyzed. Box plots are depicted solely for aquifer systems with at least three monitoring wells within a given distance interval. Light blue and blue dashed lines near the horizontal axis correspond to the Cl⁻ concentration standard of seawater intrusion (250 mg/liter) and the monitored Cl⁻ concentration of coastal seawater, respectively.

regions can be classified into three major geomorphic units, i.e., coastal plains, hilly and low-mountain coastal zones, and mountainous coastal zones. The coastal plains include Liaodong Bay, Bohai Bay, Laizhou Bay, and North Jiangsu. The hilly and low-mountain coastal areas are placed along shorelines such as Qinhuangdao, Longkou, and the Dagu River estuary, whereas the mountainous coastal areas are associated with the seawater intrusion documented along the banks of the Zhujiang River in Guangdong Province.

Coastal plains

Coastal plains are mainly distributed in Northeast China, North China, and North Jiangsu. These are characterized by thick substantial sedimentary deposits (200 to 800 m) of alternating marine and fluvial facies. These areas experience modest rainfall (with an annual mean precipitation of 600 to 930 mm) coupled with high evaporation rates (about 1020 to 1630 mm on average, annually). Consequently, groundwater resources are extensively used for various purposes including agriculture, industrial processes, and domestic use. Brine extraction is reported to be practiced for aquaculture (*47*). In the coastal areas of Liaodong Bay, Bohai Bay, Laizhou Bay, and North Jiangsu, a notable fraction of groundwater wells (i.e., 27.2, 70.4, 61.5, and 34.8%, respectively) is characterized by water levels lower than sea level (Fig. 2, A, C, D, and G). We recall that a landward hydraulic gradient can form even in cases where water table is close to sea level due to density differences between salt water and fresh water. Temporary underground funnel and local landward hydraulic gradients can also form when the natural water table is substantially above sea level as a consequence of inland pumping, resulting in instances of ancient saltwater intrusion. For instance, one can see that a substantial and continuous groundwater funnel has formed in the coastal region of Bohai Bay (Fig. 2C). This has induced the intrusion of ancient salt water from the shoreline into the inland areas, reaching a distance of about 90 km from the coastline. As a result, the median concentration of Cl⁻ is greater than 250 mg/liter within each 10-km interval distance according to which data in Fig. 2 are clustered. In the coastal areas of Liaodong Bay, Laizhou Bay, and North Jiangsu, multiple adjacent funnels gradually merge into large ones. This contributes to disrupting the dynamic balance between fresh water and ancient salt water within the aquifers. As a result, the salt water–fresh water interface advances inland, triggering extensive episodes of paleo-saltwater intrusion. The extent of the regions where the presence of salt water is documented has currently reached ~56.2 km in the Liaodong Bay, 135.6 km in the Jiaozhou Bay, and 87.9 km in North Jiangsu. Notably, median concentrations of Cl⁻ are lower than 250 mg/liter at distances from the shoreline corresponding to 20 to 30 km in Liaodong Bay and 30 to 40 km in Laizhou Bay. These values may be attributed to freshwater influx from rivers and canals.

Hilly and low-mountain coastal areas

Along hilly and low-mountainous coastal lines, such as Qinhuangdao (Fig. 2B), Longkou (Fig. 2E), and the Dagu River estuary (Fig. 2F). Quaternary deposits are mostly thin, often hosting unconfined aquifers with scattered clay or subclay lenses. Over a long period, recharge from rainfall and surface water tends to reduce persistence of ancient salt water. Otherwise, overpumping for agriculture near river estuaries has contributed to lower groundwater levels and to form landward hydraulic gradients. In these regions, 71.2, 86.5, and 69.5% of wells are characterized by water levels below sea level, so that seawater intrusion is enhanced. In Qinhuangdao, Longkou, and the Dagu River estuary, intrusion typically extends 10 to 20 km inland, Cl^- concentration declining sharply away from the coast.

Mountainous areas: Scattered intrusion in Southern China

In Southern China, regions such as Zhejiang, Fujian, Guangxi, Hainan, and parts of Guangdong provinces exhibit only scattered saltwater intrusion (*48*). High annual rainfall, notable topographic relief, and rocky coastlines contribute to substantial freshwater recharge and maintain high water tables, thus inducing seaward hydraulic gradients. These natural features limit the extent of seawater intrusion. As such, they offer a degree of resilience that is not observed in the northern plains. Tide-driven seawater upflow along rivers represents an important mechanism of modern seawater intrusion. For instance, along the Zhujiang River in Guangdong Province, such upflow has induced intrusion extending ~20 km inland on both riverbanks (Fig. 2H). This intrusion pattern, combined with declining water levels, underscores the vulnerability of these regions to salinization (*49*).

Contribution of paleo–salt water to seawater intrusion

The hydrochemical composition of groundwater is imprinted by its recharge sources and prevailing hydrogeological conditions (*45*, *50*, *51*). Groundwater isotopic characteristics offer critical insights into recharge origins and geochemical processes such as leaching, evaporation, and mixing (*44*, *52*). Whereas atmospheric precipitation and rivers constitute primary recharge sources for aquifers, seawater also contributes to recharge in coastal areas. Monitoring of groundwater quality across representative study areas (including Liaodong bay, Qinhuangdao, Bohai bay, Laizhou Bay, Dagu River estuary, Longkou, North Jiangsu, and banks of Zhujiang River) reveals distinct patterns in $\delta^{18}O$ (*53*), with values increasing from inland recharge zones to coastal discharge regions (table S2). Notably, $\delta^{18}O$ content in brine [−4.39 per mil (‰)] is significantly lower than its counterpart detected in seawater (−0.50‰). We note that here we rely on $\delta^{18}O$ and Cl^- concentrations to differentiate between modern seawater intrusion and paleo–salt water (*45*, *54*). Consistent with our approach, we then evaluate mixing curves for seawater and groundwater samples with the highest salt concentrations. These are depicted as blue and red dotted curves in Fig. 3, respectively.

Concentrations of Cl^- in unconfined aquifers were consistently lower than those in nearby seawater (Fig. 3, B, E, F, and H). Mixing curves for seawater and groundwater samples with the highest salt concentrations are seen to largely overlap, values of the deviation ratio being approximately equal to unity. These observations confirm the occurrence of modern seawater intrusion. Inland freshwater points (light blue symbols in Fig. 3) are located above the mixing curves, suggesting differing degrees of leaching in these regions. Otherwise, sampling wells corresponding to brackish and saltwater data (green and dark blue symbols in Fig. 3) exhibit fluctuations due to evaporation, ion exchange, and precipitation. Processes such as surface evaporation from shallow aquifers caused an enrichment of heavy isotopes ($\delta^{18}O$) as lighter isotopes ($\delta^{16}O$) were preferentially removed during evaporation. Simultaneously, cation exchange between calcium ions (Ca^{2+}) in fresh groundwater and sodium ions (Na^+) in salt water favored precipitation of isotopically heavier minerals such $CaC^{18}O_3$ and $CaMg(C^{18}O_3)_2$, thus contributing to reducing $\delta^{18}O$ in saltwater areas.

Concentrations of Cl^- in coastal plains (including Liaodong Bay, Bohai Bay, Laizhou Bay, and North Jiangsu; Fig. 3, A, C, D, and G), were exceptionally high, attaining values far exceeding nearby seawater concentrations, i.e., 36,637.00, 25,653.00, 96,067.92, and 27,674.73 mg/liter, respectively. These samples deviated significantly from seawater and paleo-saltwater mixing lines, being associated with deviation ratios equal to 3.77, 1.71, 46.65, and 1.94, respectively. Such deviations offer a strong indication of paleo-saltwater intrusion. Samples associated with monitoring well corresponding to unconfined aquifers lie above mixing curves (Fig. 3). This suggests that these aquifers have minimal interaction with impermeable layers, allowing for more direct mixing with surface water or groundwater associated with the other permeable layers. Brackish and saline groundwater, stored in both phreatic and confined aquifers, showed contributions from atmospheric recharge and lateral inflow of paleo–salt water (Fig. 3). Processes such as surface evaporation and isotopic fractionation contributed to further enrich the presence of heavy isotopes ($\delta^{18}O$) in confined aquifers (*55*, *56*). Isotopic changes through denitration and decarbonization also enhanced $\delta^{18}O$ in these closed systems. Some occurrences of saline groundwater, particularly in Tianjin and Jiangsu (Fig. 3, C and G), appeared to be concentrated along seawater mixing lines (*45*). However, the presence of ancient salt water that is distributed continuously along such coastlines makes it difficult to unambiguously distinguish between modern and paleo-saltwater intrusion. Paleo-saltwater intrusion is characterized by the presence of (i) thick Quaternary sediments in coastal plains, (ii) groundwater Cl^- concentrations exceeding those of nearby seawater, and (iii) deviation ratios markedly larger than unity (often exceeding 1.5).

The Br/Cl ratio provides a reliable tracer for distinguishing the origin and evolutionary pathways of groundwater, thus enabling the identification of processes such as evaporation and mineral precipitation (*57*, *58*). Mixing curves were constructed using seawater (or the most saline groundwater) and the freshest groundwater sample as endmembers (fig. S1). Groundwater quality monitoring in representative coastal systems (e.g., Liaodong Bay, Bohai Bay, Longkou, and banks of Zhujiang River) reveals systematic increases in Br/Cl values from inland recharge areas toward coastal discharge zones. In the coastal area of Liaodong Bay, most groundwater samples (fresh and brackish) are located above the seawater mixing line due to evaporation and mineral precipitation processes. The clear separation between the seawater and brine mixing lines provides strong evidence for the presence of paleo-saltwater intrusion in Liaodong Bay and Bohai Bay. Meanwhile, the Br/Cl values of some groundwater samples exceed the range of modern seawater, further demonstrating that groundwater has been influenced by paleo-saltwater intrusion (fig. S1, A and B). Sampling points from the unconfined aquifer cluster along these mixing trajectories, which nearly overlap, thereby supporting the occurrence of modern seawater intrusion. Notably, most freshwater and brackish samples are located below the mixing lines (fig. S1, C and D), suggesting that groundwater samples have experienced varying degrees of leaching from precipitation or surface water. Otherwise, a smaller subset of freshwater and brackish samples are located above the mixing trajectories, consistent with effects of evaporation and mineral precipitation.

In summary, isotopic, Cl^- concentration and ion ratio analyses suggest the action of two dominant types of seawater intrusion in China: modern seawater intrusion and paleo-saltwater intrusion (Fig. 3).

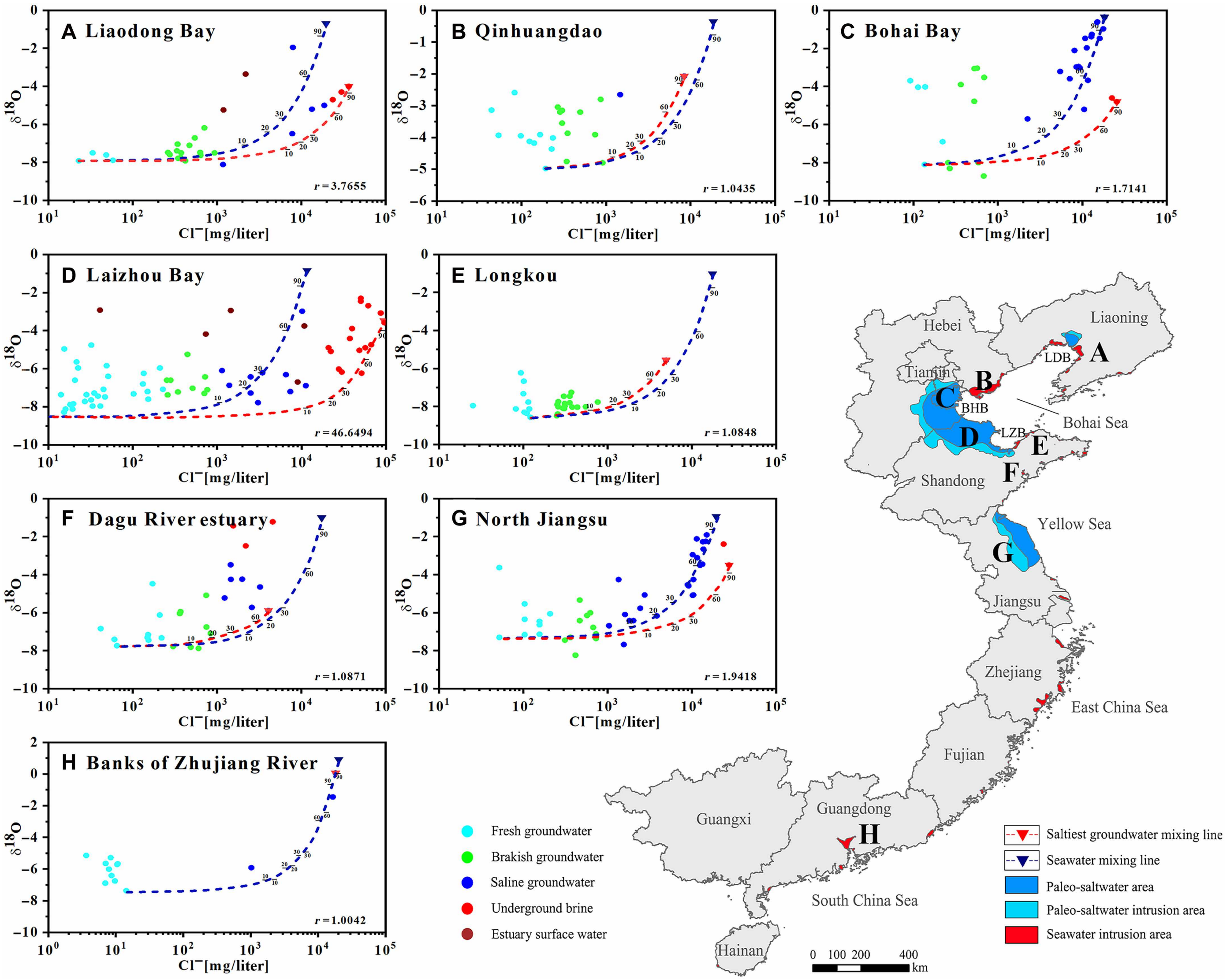

Fig. 3. Distributions of modern seawater intrusion and paleo-saltwater intrusion regions in China. Subpanels (**A** to **H**) show the relationship curves between $\delta^{18}O$ and Cl^-, as well as the distribution of groundwater samples in each area. In these plots, the freshest groundwater sample is considered the low-concentration end, whereas offshore seawater and the saltiest groundwater samples serve as the high-concentration ends, respectively. Groundwater samples are classified into fresh (<250 mg/liter), brackish (250 to 1000 mg/liter), or saline groundwater (1000 to 19,400 mg/liter) and subsurface brine (>19,400 mg/liter).

Whereas modern seawater intrusion takes place only locally in coastal plains, paleo-saltwater intrusion dominates. Our comprehensive analyses reveal that paleo-saltwater intrusion affects about 23,100 km^2 (about 66% of the total affected area), whereas modern seawater intrusion spans about 12,000 km^2 (about 34%) (table S3). Seawater intrusion is most pronounced in Northern China, including Liaoning (3316.42 km^2), Hebei (8340.55 km^2), Tianjin (1394.66 km^2), Shandong (9347.64 km^2), and North Jiangsu (7868.56 km^2), collectively accounting for 86.2% of the total affected area.

Summary and outlook

We present the nationwide investigation of seawater intrusion along China's coastline, highlighting the crucial role of paleo–salt water in influencing salinity patterns in coastal aquifers. By analyzing over 2100 groundwater samples and conducting geophysical and geochemical surveys, we identify a clear correlation between seawater intrusion and tectonic subsidence zones, with paleo-saltwater intrusion affecting 66% of the observed salinized areas. In contrast, modern seawater intrusion, which is primarily observed in hilly, low-mountain, and mountain regions with thinner sediments, accounts for 34%. Geochemical analysis (specifically $\delta^{18}O$ and Cl^- concentrations) further enables to distinguish these two sources, linking paleo–salt water to Quaternary sea level fluctuations and evaporation processes.

Our growing knowledge over the past decade shows the importance of understanding the geochemical processes that govern seawater intrusion, revealing distinct dynamics between paleo–salt water and modern seawater. Our findings include that paleo–salt water is largely confined to coastal plains with thick Quaternary sediments, where it contributes to salinity levels exceeding those of nearby seawater. In contrast, modern seawater intrusion primarily occurs in areas with unconfined aquifers and thinner sediments, such as coastal hilly and mountainous regions. These findings offer crucial insights into the mechanisms of seawater intrusion, providing a robust framework for managing salinity in coastal aquifers, both in China and globally.

Recognizing the fundamental role of paleo–salt water contributes to reshape groundwater management priorities at a fundamental level. Whereas modern seawater intrusion can often be mitigated through localized interventions such as pumping reductions or engineered barriers, addressing paleo-saltwater intrusion requires coordinated, basin-scale strategies aimed at restoring groundwater levels, restricting deep-well development, and reallocating freshwater resources. This distinction is markedly critical for developing regions with limited water and financial resources.

Our findings underscore that dominance of paleo–salt water in China's coastal plains bears the signature of a broader global pattern. Comparable Quaternary sedimentary basins are found in vulnerable deltas such as the Ganges-Brahmaputra, Nile, and Mekong, where thick marine-fluvial sequences and past sea level fluctuations have entrapped saline waters. In these regions, groundwater is a critical resource for dense populations. Yet, salinization is frequently misattributed to modern seawater intrusion. The diagnostic framework we present provides a low-cost, accessible tool (based on metrics such as Cl^- thresholds and $\delta^{18}O$ deviations) to identify paleo–salt water in contexts lacking advanced monitoring infrastructure.

Future research should address the long-term impacts of paleo-saltwater and modern seawater intrusion on groundwater resources, particularly under intensified climate change and human activities (*59*). Developing more effective management strategies for coastal aquifers, especially in regions with extensive paleo-saltwater intrusion, is crucial to mitigating salinization risks. In addition, broader integration of isotopic and hydro-chemical methods can deepen our understanding of seawater intrusion patterns worldwide, providing valuable guidance for global water resource management and policy.

MATERIALS AND METHODS

Sampling and analysis

From November 2019 to February 2020 (with the exception of water samples from the Dagu River Estuary and Longkou areas collected in November to December 2017), we designed and implemented an extensive field investigation encompassing hydrogeological surveys and sample collection to assess seawater intrusion along China's coasts. This investigation was conducted by the Observation and Research Station of Seawater Intrusion and Soil Salinization, Ministry of Natural Resources, China, as part of a joint field investigation and monitoring program with the Ocean University of China and the First Institute of Oceanography, Ministry of Natural Resources. The sample collection was supported by the National Key R&D Plan of China (grant no. 2016YFC0402801). No specific permits were required for the sampling at these locations as the sites are open to public access and do not fall within protected areas or involve endangered species. All sampling activities complied with local environmental regulations. This effort involved the collection of groundwater samples from over 2100 wells. It has primarily focused on shallow aquifers at depths ranging from 6 to 81 m. These samples included measurements of water table depth and chloride (Cl^-) concentrations (table S1). More than 500 of these samples are also analyzed for isotope ($\delta^{18}O$) and Cl^- concentrations. The selection of the 500 samples for isotope analysis was based on the following principles to ensure representativeness. First, the preliminary distributions of paleo–salt water and saline water were determined according to existing hydrogeological data such as drilling records and hydrogeological survey data. Then, 2100 groundwater monitoring wells were selected to determine the actual distribution range of saline water areas by measuring groundwater quality, including salinity and chloride ions. On this basis, the 500 isotope monitoring points were chosen to cover both seawater intrusion zones and paleo-saltwater intrusion zones along the national coast. Each monitoring section included at least three monitoring points, encompassing freshwater endmembers, seawater or paleo-saltwater endmembers, and samples from the saline-freshwater mixing zone.

In cases of monitoring wells featuring multiple water level measurements, only the median of all data is included in the final curated dataset. To assist our analysis of the dynamic features and spatial distribution of salinity associated with seawater intrusion, we depict the distributions of main lithological type, paleo–salt water, and sampling wells across the coastal region. Each water sample was filtered through a 0.45-μm polyethersulfone (PES) filter membrane (diameter of 25 mm) for ionic analysis and stored in precleaned polyethylene containers. To minimize contamination, containers were sealed with tape to isolate them from the atmosphere. Samples were refrigerated at temperatures below 4°C until analysis. Groundwater levels were measured using portable water-level monitors. Cl^- concentrations were determined using an ion chromatograph (ICS 3000) with an analytical precision of ±0.05 mg/liter, whereas $\delta^{18}O$ was measured using an Los Gatos Research liquid water isotope laser mass spectrometer at the Nanjing Hydraulic Research Institute. The values of $\delta^{18}O$ were calculated relative to VSMOW (Vienna standard mean ocean water) with an analytical precision of ±0.2‰. All $\delta^{18}O$ values are reported in δ units.

Calculation of deviation ratio

To differentiate between modern seawater intrusion and paleo-saltwater intrusion, the relationships between Cl^- concentration and $\delta^{18}O$ were analyzed using mixing curves. Semilogarithmic coordinates were transformed into Cartesian systems, generating two linear functions

$$f_1(x) = a_1 x + b_1 \tag{1}$$

$$f_2(x) = a_2 x + b_2 \tag{2}$$

where $f_1(x)$ and $f_2(x)$ represent the calculated $\delta^{18}O$ isotope concentration for the seawater mixing curve and the highest-salinity groundwater mixing curve, respectively; a_i and b_i are constants for $i = 1, 2$.

The deviation of a given sample set SS [where each sample is represented as a pair (s_i, s_j), indicating Cl^- and $\delta^{18}O$ concentrations, respectively] from these curves was quantified through the mean square error (MSE)

$$\mathrm{MSE}_k = E\left\{\left[s_j - f_k\left(s_i\right)\right]^2\right\} = \frac{1}{N}\sum_{n=1}^{N}\left[s_j - f_k\left(s_i\right)\right]^2 \tag{3}$$

where N is the number of samples in SS, $k = 1, 2$ refers to the seawater and saltwater mixing curves, respectively, and E is the expectation.

The deviation ratio r of the relationship curves between $\delta^{18}O$ and Cl^- is then defined as

$$r = \frac{\mathrm{MSE}_2}{\mathrm{MSE}_1} \tag{4}$$

where MSE_2 and MSE_1 represent the MSEs for seawater and paleo-saltwater mixing curves, respectively, which quantify the overall extent of deviation of groundwater samples from these mixing lines. When $r \approx 1$, the mixing curves overlap closely, indicating modern seawater intrusion. Conversely, when $r \gg 1$, the separation between the curves in the high-salinity range suggests the presence of high-salinity ancient saltwater or brine intrusion.

Supplementary Materials

This PDF file includes:
Fig. S1
Tables S1 to S3

REFERENCES

1. B. Stewart-Koster, S. E. Bunn, P. Green, C. Ndehedehe, L. S. Andersen, D. I. Armstrong McKay, X. Bai, F. DeClerck, K. L. Ebi, C. Gordon, J. Gupta, S. Hasan, L. Jacobson, S. J. Lade, D. Liverman, S. Loriani, A. Mohamed, N. Nakicenovic, D. Obura, D. Qin, C. Rammelt, J. C. Rocha, J. Rockström, P. H. Verburg, C. Zimm, Living within the safe and just Earth system boundaries for blue water. *Nat. Sustain.* **7**, 53–63 (2024).
2. M. Thaw, M. GebreEgziabher, J. Y. Villafañe-Pagán, S. Jasechko, Modern groundwater reaches deeper depths in heavily pumped aquifer systems. *Nat. Commun.* **13**, 5263 (2022).
3. S. Jasechko, D. Perrone, H. Seybold, Y. Fan, J. W. Kirchner, Groundwater level observations in 250,000 coastal US wells reveal scope of potential seawater intrusion. *Nat. Commun.* **11**, 3229 (2020).
4. X. Kuang, J. Liu, B. R. Scanlon, J. J. Jiao, S. Jasechko, M. Lancia, B. K. Biskaborn, Y. Wada, H. Li, Z. Zeng, Z. Guo, Y. Yao, T. Gleeson, J.-P. Nicot, X. Luo, Y. Zou, C. Zheng, The changing nature of groundwater in the global water cycle. *Science* **383**, eadf0630 (2024).
5. E. Luijendijk, T. Gleeson, N. Moosdorf, Fresh groundwater discharge insignificant for the world's oceans but important for coastal ecosystems. *Nat. Commun.* **11**, 1260 (2020).
6. C. M. Richardson, K. L. Davis, C. Ruiz-González, J. A. Guimond, H. A. Michael, A. Paldor, N. Moosdorf, A. Paytan, The impacts of climate change on coastal groundwater. *Nat. Rev. Earth Environ.* **5**, 100–119 (2024).
7. J. Yin, N. Wang, C. Lu, F. T. C. Tsai, H. Chen, Fast desalinization of residual saltwater using subsurface dams combined with saltwater discharge or freshwater recharge. *J. Hydrol.* **619**, 129282 (2023).
8. M. Ono, I. Machida, M. Koshigai, R. Ikawa, A. Marui, Vertical distribution of groundwater age in and around the freshwater–saltwater transition zone determined using noble gases and carbon isotopes. *J. Hydrol.* **627**, 130353 (2023).
9. A. H. Sawyer, C. H. David, J. S. Famiglietti, Continental patterns of submarine groundwater discharge reveal coastal vulnerabilities. *Science* **353**, 705–707 (2016).
10. H. Xiao, Y. Tang, H. Li, L. Zhang, T. Ngo-Duc, D. Chen, Q. Tang, Saltwater intrusion into groundwater systems in the Mekong Delta and links to global change. *Adv. Clim. Chang. Res.* **12**, 342–352 (2021).
11. F. Wang, X. Li, X. Tang, X. Sun, J. Zhang, D. Yang, L. Xu, H. Zhang, H. Yuan, Y. Wang, Y. Yao, C. Wang, Y. Guo, Q. Ren, Y. Li, R. Zhang, X. Wang, B. Zhang, Z. Sha, The seas around China in a warming climate. *Nat. Rev. Earth Environ.* **4**, 535–551 (2023).
12. D. Han, M. J. Currell, G. Cao, B. Hall, Alterations to groundwater recharge due to anthropogenic landscape change. *J. Hydrol.* **554**, 545–557 (2017).
13. C. Liu, P. Li, D. Liu, Prevent coastal seawater intrusion in China. *Science* **388**, 258–258 (2025).
14. Q. Zhou, J. Zhang, S. Zhang, Q. Chen, H. Fan, C. Cao, Y. Zhang, Y. Yang, J. Luo, Y. Yao, Groundwater quality evolution across China. *Nat. Commun.* **16**, 2522 (2025).
15. A. P. Barker, R. J. Newton, S. H. Bottrell, J. H. Tellam, Processes affecting groundwater chemistry in a zone of saline intrusion into an urban sandstone aquifer. *Appl. Geochem.* **13**, 735–749 (1998).
16. P. M. Barlow, E. G. Reichard, Saltwater intrusion in coastal regions of North America. *Hydrgeol. J.* **18**, 247–260 (2010).
17. L. Shi, J. J. Jiao, Seawater intrusion and coastal aquifer management in China: A review. *Environ. Earth Sci.* **72**, 2811–2819 (2014).
18. J. Yang, H. Li, P. Shi, Z. Hu, Y. Hu, Q. Xu, M. L. Du D, Research status and discussion on the method of seawater intrusion in the key section of Circum-Bohai-Sea region. *Geol. Surv. Res.* **37**, 294–299 (2014).
19. F. Larsen, L. V. Tran, H. Van Hoang, L. T. Tran, A. V. Christiansen, N. Q. Pham, Groundwater salinity influenced by Holocene seawater trapped in incised valleys in the Red River delta plain. *Nat. Geosci.* **10**, 376–381 (2017).
20. V. E. A. Post, H. Van der Plicht, H. A. J. Meijer, The origin of brackish and saline groundwater in the coastal area of the Netherlands. *Neth. J. Geosci.* **82**, 133–147 (2003).
21. O. Sivan, Y. Yechieli, B. Herut, B. Lazar, Geochemical evolution and timescale of seawater intrusion into the coastal aquifer of Israel. *Geochim. Cosmochim. Acta* **69**, 579–592 (2005).
22. G. A. Harrington, W. P. Gardner, T. J. Munday, Tracking groundwater discharge to a large river using tracers and geophysics. *Groundwater* **52**, 837–852 (2014).
23. C. Sheng, J. J. Jiao, J. Zhang, Y. Yao, X. Luo, S. Yu, Y. Ni, S. Wang, R. Mao, T. Yang, L. Zhan, Evolution of groundwater system in the Pearl River Delta and its adjacent shelf since the late Pleistocene. *Sci. Adv.* **10**, eadn3924 (2024).
24. X. Dang, M. Gao, Z. Wen, G. Hou, H. Jakada, D. Ayejoto, Q. Sun, Saline groundwater evolution in the Luanhe River delta (China) during the Holocene: Hydrochemical, isotopic, and sedimentary evidence. *Hydrol. Earth Syst. Sci.* **26**, 1341–1356 (2022).
25. V. A. Bracchi, R. Nalin, D. Basso, Paleoecology and dynamics of coralline dominated facies during a Pleistocene transgressive–regressive cycle (Capo Colonna marine terrace, Southern Italy). *Palaeogeogr. Palaeoclimatol. Palaeoecol.* **414**, 296–309 (2014).
26. B. M. S. Giambastiani, N. Colombani, M. Mastrocicco, M. D. Fidelibus, Characterization of the lowland coastal aquifer of Comacchio (Ferrara, Italy): Hydrology, hydrochemistry and evolution of the system. *J. Hydrol.* **501**, 35–44 (2013).
27. F. Ding, T. Yamashita, H. S. Lee, Atmosphere-ocean-groundwater modeling system for seawater intrusion simulation in Liaodong Bay coastal plain, China. *Adv. Mater. Res.* **518-523**, 4155–4160 (2012).
28. M. Gao, G. Hou, F. Guo, Conceptual model of underground brine formation in the silty coast of Laizhou Bay, Bohai Sea, China. *J. Coastal Res.* **74**, 157–165 (2016).
29. F. Yang, S. Liu, C. Jia, M. Gao, W. Chang, Y. Wang, Hydrochemical characteristics and functions of groundwater in southern Laizhou Bay based on the multivariate statistical analysis approach. *Estuar. Coast. Shelf Sci.* **250**, 107153 (2021).
30. G. Hou, F. Yang, S. Liu, M. Gao, Q. Fan, C. Jia, Y. Liu, The characteristics of saline submarine groundwater environment on a continental shelf: An example from the south of Laizhou Bay, China. *Cont. Shelf Res.* **229**, 104557 (2021).
31. D. Han, M. J. Currell, Review of drivers and threats to coastal groundwater quality in China. *Sci. Total Environ.* **806**, 150913 (2022).
32. Z. Zhou, G. Zhang, M. Yan, J. Wang, Spatial variability of the shallow groundwater level and its chemistry characteristics in the low plain around the Bohai Sea, North China. *Environ. Monit. Assess.* **184**, 3697–3710 (2012).
33. X. Xu, G. Xiong, G. Chen, T. Fu, H. Yu, J. Wu, W. Liu, Q. Su, Y. Wang, S. Liu, X. Shi, Characteristics of coastal aquifer contamination by seawater intrusion and anthropogenic activities in the coastal areas of the Bohai Sea, eastern China. *J. Asian Earth Sci.* **217**, 104830 (2021).
34. D. Han, C. Kohfahl, X. Song, G. Xiao, J. Yang, Geochemical and isotopic evidence for palaeo-seawater intrusion into the south coast aquifer of Laizhou Bay, China. *Appl. Geochem.* **26**, 863–883 (2011).
35. Y. Du, T. Ma, L. Chen, H. Shan, C. Xiao, Y. Lu, C. Liu, H. Cai, Genesis of salinized groundwater in Quaternary aquifer system of coastal plain, Laizhou Bay, China: Geochemical evidences, especially from bromine stable isotope. *Appl. Geochem.* **59**, 155–165 (2015).
36. M. Gao, Q. Sun, X. Dang, G. Hou, F. Guo, Z. Liu, X. Chang, G. Zhao, Hydrogeochemical characteristic and recognization of saline groundwater formation and evolution in silty coast of the Yellow Sea and Bohai Sea, Eastern China. *Front. Earth Sci.* **11**, 1186661 (2023).
37. J. Li, X. Liang, M. Jin, G. Xiao, J. He, Y. Pei, Geochemistry of clayey aquitard pore water as archive of paleo-environment, western Bohai Bay. *J. Earth Sci.* **26**, 445–452 (2015).
38. S. Yu, J. J. Jiao, X. Luo, H. Li, X. Wang, Q. Wang, M. Yao, Y. Guo, Z. Deng, J. Zuo, Vertical leaching of paleo-saltwater in a coastal aquifer–aquitard system of the Pearl River Delta. *J. Hydrol.* **626**, 130168 (2023).
39. J. Li, X. Gong, X. Liang, Y. Liu, J. Yang, X. Meng, A. Alhassan, Salinity evolution of aquitard porewater associated with transgression and regression in the coastal plain of Eastern China. *J. Hydrol.* **603**, 127050 (2021).
40. T. Zheng, X. Zheng, Q. Chang, H. Zhan, M. Walther, Timescale and effectiveness of residual saltwater desalinization behind subsurface dams in an unconfined aquifer. *Water Resour. Res.* **57**, e2020WR028493 (2021).
41. Q. Chang, T. Zheng, C. Gao, X. Zheng, Y. Lin, X. Song, M. Walther, Hydrodynamic behavior of freshwater-saltwater mixing zone in the context of subsurface physical barriers. *J. Environ. Manage.* **353**, 120080 (2024).
42. A. M. Helton, P. J. Dennedy-Frank, R. E. Emanuel, S. C. Neubauer, K. H. Adams, M. Ardon, L. Band, K. M. Befus, H. Borstlap, J. A. Duberstein, A. C. Gold, J. S. Kominoski, A. K. Manda, H. A. Michael, S. M. J. Moysey, A. N. Myers-Pigg, J. A. Neville, G. Noe, J. Panthi, E. Pezeshki, M. J. Sirianni, N. D. Ward, Over, under, and through: Hydrologic connectivity and the future of coastal landscape salinization. *Water Resour. Res.* **61**, e2024WR038720 (2025).
43. J. A. Cantelon, J. A. Guimond, C. E. Robinson, H. A. Michael, B. L. Kurylyk, Vertical saltwater intrusion in coastal aquifers driven by episodic flooding: A review. *Water Resour. Res.* **58**, e2022WR032614 (2022).
44. D. M. Han, X. F. Song, M. J. Currell, J. L. Yang, G. Q. Xiao, Chemical and isotopic constraints on evolution of groundwater salinization in the coastal plain aquifer of Laizhou Bay, China. *J. Hydrol.* **508**, 12–27 (2014).
45. G. Xiong, G. Chen, J. Wu, T. Fu, Y. Yang, X. Xu, X. Zhu, H. Yu, S. Liu, M. Gao, G. Hou, Seawater intrusion-retreat processes and groundwater evolution in intruded coastal aquifers with land reclamation: A case study of Eastern Jiangsu, China. *Lithosphere* **2021**, 1308487 (2022).

46. G. Chen, G. Xiong, J. Lin, X. Xu, H. Yu, W. Liu, T. Fu, Q. Su, Y. Wang, Y. Dai, I. Ali, X. Zheng, C. Peng, Elucidating the pollution sources and groundwater evolution in typical seawater intrusion areas using hydrochemical and environmental stable isotope technique: A case study for Shandong Province, China. *Lithosphere* **2021**, 4227303 (2021).
47. C.-H. Lee, H.-J. Ho, W.-S. Chen, A. Iizuka, Total resource circulation of desalination brine: A review. *Adv. Sustain. Syst.* **8**, 2300460 (2024).
48. G. Xiong, G. Chen, J. Wu, Z. Wang, H. Yu, T. Fu, W. Liu, X. Xu, G. Hou, Y. Yang, X. Zhu, Identifying the characteristics and potential risk of seawater intrusion for southern China by the SBM-DEA model. *Sci. Total Environ.* **844**, 157205 (2022).
49. M. C. Hingst, R. M. Housego, C. He, B. J. Minsley, L. B. Ball, H. A. Michael, Beyond the wedge: Impact of tidal streams on salinization of groundwater in a coastal aquifer stressed by pumping and sea-level rise. *Water Resour. Res.* **60**, e2023WR035840 (2024).
50. D. Han, M. J. Currell, Delineating multiple salinization processes in a coastal plain aquifer, northern China: Hydrochemical and isotopic evidence. *Hydrol. Earth Syst. Sci.* **22**, 3473–3491 (2018).
51. Y. Zhang, M. Wang, J. Peñuelas, J. Xue, Z. Huang, X. Gou, N. G. McDowell, Coastal groundwater salinization impairs tree carbon–water balance. *Commun. Earth Environ.* **496**, 1049 (2025).
52. C. Sheng, J. J. Jiao, X. Luo, J. Zuo, L. Jia, J. Cao, Offshore freshened groundwater in the Pearl River estuary and shelf as a significant water resource. *Nat. Commun.* **14**, 3781 (2023).
53. T. Fu, C. Li, Z. Wang, C. Qi, G. Chen, Y. Fu, Q. Su, X. Xu, W. Liu, H. Yu, Hydrochemical characteristics and quality assessment of groundwater in Guangxi coastal areas, China. *Mar. Pollut. Bull.* **188**, 114564 (2023).
54. S. Liu, Z. Tang, M. Gao, G. Hou, Evolutionary process of saline-water intrusion in Holocene and Late Pleistocene groundwater in southern Laizhou Bay. *Sci. Total Environ.* **607-608**, 586–599 (2017).
55. A. Gibrilla, J. R. Fianko, S. Ganyaglo, D. Adomako, G. Anornu, N. Zakaria, Nitrate contamination and source apportionment in surface and groundwater in Ghana using dual isotopes (^{15}N and ^{18}O-NO_3) and a Bayesian isotope mixing model. *J. Contam. Hydrol.* **233**, 103658 (2020).
56. Y.-Y. Zhao, Y.-F. Zheng, Stable isotope evidence for involvement of deglacial meltwater in Ediacaran carbonates in South China. *Chem. Geol.* **271**, 86–100 (2010).
57. M. L. Kirwan, H. A. Michael, K. B. Gedan, K. L. Tully, S. Fagherazzi, N. G. McDowell, G. D. Molino, D. Pratt, W. G. Reay, S. Stotts, Feedbacks regulating the salinization of coastal landscapes. *Ann. Rev. Mar. Sci.* **17**, 461–484 (2025).
58. S. Yu, J. J. Jiao, X. Luo, H. Li, X. Wang, X. Zhang, M. Yao, J. Zuo, W. Liang, M. Lu, Evolutionary history of the groundwater system in the Pearl River Delta (China) during the Holocene. *Geology* **51**, 481–485 (2023).
59. E. Rignot, E. Ciracì, B. Scheuchl, V. Tolpekin, M. Wollersheim, C. Dow, Widespread seawater intrusions beneath the grounded ice of Thwaites Glacier, West Antarctica. *Proc. Natl. Acad. Sci. U.S.A.* **121**, e2404766121 (2024).
60. Z. Sun, X. Song, H. Bu, L. Yang, Y. Ma, Y. Zhang, D. Han, Origin of groundwater salinity and hydrochemical processes in an unconfined aquifer: Case of Yang-Dai River basin in Qinhuangdao (China). *Environ. Earth Sci.* **75**, 54 (2015).
61. Z. Zhang, H. Zhang, J. Sun, L. Yang, Y. Cui, L. Wu, J. Qi, J. Xu, Environmental isotope study related to groundwater age, flow system and saline water origin in Quaternary aquifer of Hebei Plain. *Hydrogeol. Eng. Geol.* **4**, 1–6 (1987).
62. J. Wu, F. Meng, X. Wang, D. Wang, The development and control of the seawater intrusion in the eastern coastal of Laizhou Bay, China. *Environ. Geol.* **54**, 1763–1770 (2008).
63. B. Zhang, T. Zheng, X. Zheng, M. Walther, Utilization of pit lake on the cleaning process of residual saltwater in unconfined coastal aquifers. *Sci. Total Environ.* **770**, 144670 (2021).
64. J. Liu, "Hydrochemical evolution mechanism and optimization of monitoring network for groundwater in Pearl River Delta," thesis, Northwest University, Xi'an, SN (2020).

Acknowledgments

Funding: This work was supported by the National Natural Science Foundation of China (grant no. 42422207 to T.Z. and grant no. U1806210 to X.Z.), the National Key Research and Development Program of China (grant no. 2016YFC0402810 to X.Z.), and the European Union Next-Generation EU [National Recovery and Resilience Plan (NRRP), Mission 4, Component 2, Investment 1.3, D.D. no. 1243 (2/8/2022), PE0000005] in the context of the RETURN Extended Partnership for A.G. **Author contributions:** Conceptualization: T.Z., X.Z., J.W., G.C., J.Li., C.Z., and J.Lu. Methodology: T.Z., B.G., Q.S., X.Z., J.Lu., and A.G. Investigation: Q.C., Q.S., Z.Z., S.G., and B.Z. Visualization: T.Z., B.G., X.C., X.Z., Z.Z., S.G., D.W., T.L., and X.X. Funding acquisition: T.Z., X.Z., and A.G. Project administration: T.Z., X.Z., and A.G. Supervision: X.Z., J.W., G.C., J.Lu. and A.G. Writing—original draft: T.Z., X.Z., J.Lu. and A.G. Writing—review and editing: B.G., X.C., X.Z., S.G., J.W., C.Z., T.L., X.L., X.X., J.Li., G.C., L.Z., Y.W., O.K., J.Lu., and A.G. Resources: X.L. Data curation: X.L. Validation: X.L. **Competing interests:** The authors declare that they have no competing interests. **Data, code, and materials availability:** This study did not generate new materials. All data and code needed to evaluate and reproduce the results in the paper are present in the paper and/or the Supplementary Materials. The data for this study have been deposited in the database Zenodo: https://doi.org/10.5281/zenodo.18417421.

Submitted 12 May 2025
Accepted 21 April 2026
Published 20 May 2026
10.1126/sciadv.ady2322

Paleo–salt water dominates coastal aquifer salinization: A continental-scale study in China

Tianyuan Zheng, Bo Guo, Qinpeng Chang, Qiguo Sun, Xiaogang Chen, Xilai Zheng, Jichun Wu, Zhihong Zheng, Shaobo Gao, Chunmiao Zheng, Junguo Liu, Dong Wang, Tao Liu, Xiaolei Liu, Guangquan Chen, Xingyong Xu, Bo Zhang, Lin Zhang, Yajie Wu, Olaf Kolditz, Jian Luo, and Alberto Guadagnini

Sci. Adv. **12** (21), eady2322. DOI: 10.1126/sciadv.ady2322

Science Advances (ISSN 2375-2548) is published by the American Association for the Advancement of Science. 1200 New York Avenue NW, Washington, DC 20005. The title *Science Advances* is a registered trademark of AAAS.